Journal of the Endocrine Society, 2022, **6**, 1–10
https://doi.org/10.1210/jendso/bvac025
Advance access publication 18 February 2022
Clinical Research Article

Functional Assessment of Calcium-Sensing Receptor Variants Confirms Familial Hypocalciuric Hypercalcemia

Benjamin H. Mullin,[1,2] Nathan J. Pavlos,[2] Suzanne J. Brown,[1] John P. Walsh,[1,3] Ross A. McKellar,[1] Scott G. Wilson,[1,2,4] and Bryan K. Ward[1,5]

[1]Department of Endocrinology and Diabetes, Sir Charles Gairdner Hospital, Nedlands, WA 6009, Australia
[2]School of Biomedical Sciences, University of Western Australia, Nedlands, WA 6009, Australia
[3]Medical School, University of Western Australia, Nedlands, WA 6009, Australia
[4]Department of Twin Research and Genetic Epidemiology, King's College London, London WC2R 2LS, UK
[5]Harry Perkins Institute of Medical Research, Centre for Medical Research, QEII Medical Centre, University of Western Australia, Nedlands, WA 6009, Australia

Correspondence: Dr. Bryan K. Ward, Department of Endocrinology and Diabetes, Block C, Level 1, Sir Charles Gairdner Hospital, Hospital Avenue, Nedlands, WA 6009, Australia. Email: bryan.ward@perkins.uwa.edu.au.

Abstract

Context: In the clinic it is important to differentiate primary hyperparathyroidism (PHPT) from the more benign, inherited disorder, familial hypocalciuric hypercalcemia (FHH). Since the conditions may sometimes overlap biochemically, identification of calcium-sensing receptor (*CASR)* gene variants causative of FHH (but not PHPT) is the most decisive diagnostic aid. When novel variants are identified, bioinformatics and functional assessment are required to establish pathogenicity.

Objective: We identified 3 novel *CASR* transmembrane domain missense variants, Thr699Asn, Arg701Gly, and Thr808Pro, in 3 probands provisionally diagnosed with FHH and examined the variants using bioinformatics and functional analysis.

Methods: Bioinformatics assessment utilized wANNOVAR software. For functional characterization, each variant was cloned into a mammalian expression vector; wild-type and variant receptors were transfected into HEK293 cells, and their expression and cellular localization were assessed by Western blotting and confocal immunofluorescence, respectively. Receptor activation in HEK293 cells was determined using an IP-One ELISA assay following stimulation with Ca^{++} ions.

Results: Bioinformatics analysis of the variants was unable to definitively assign pathogenicity. Compared with wild-type receptor, all variants demonstrated impaired expression of mature receptor reaching the cell surface and diminished activation at physiologically relevant Ca^{++} concentrations.

Conclusion: Three *CASR* missense variants identified in probands provisionally diagnosed with FHH result in receptor inactivation and are therefore likely causative of FHH. Inactivation may be due to inadequate processing/trafficking of mature receptor and/or conformational changes induced by the variants affecting receptor signaling. This study demonstrates the value of functional studies in assessing genetic variants identified in hypercalcemic patients.

Key Words: familial hypocalciuric hypercalcemia, calcium-sensing receptor variants, functional assessment, IP-One ELISA assay, receptor expression, immunofluorescence

Abbreviations: *AP2S1*, adaptor-related protein complex 2, sigma 1 subunit (gene); CADD, combined annotation dependent depletion (score); CaSR, calcium-sensing receptor (protein); *CASR*, calcium-sensing receptor (gene); DMEM, Dulbecco's Modified Eagle Medium; EC_{50}, concentration of Ca++ ions giving half maximal % stimulation; ELISA, enzyme-linked immunosorbent assay; ER, endoplasmic reticulum; FHH, familial hypocalciuric hypercalcemia; GM130, Golgi matrix protein of 130 kDa; *GNA11*, G-protein subunit α-11 (gene); GPCR, G protein coupled receptor; ICL, intracellular loop; PDI, protein disulfide-isomerase; PHPT, primary hyperparathyroidism; PTH, parathyroid hormone; SEM, standard error of the mean; TM, transmembrane.

Familial hypocalciuric hypercalcemia (FHH) is an autosomal dominant inherited disorder in which affected individuals experience lifelong, mild to moderate elevations in serum calcium but with unsuppressed parathyroid hormone (PTH) levels and inappropriately low urine calcium levels [1-3]. The condition is generally asymptomatic and treatment is not usually indicated [2, 3]. Most cases (~65%) are caused by inactivating variants in the calcium-sensing receptor gene (*CASR*) (FHH-1), while others (~6%) can be attributed to inactivating variants in the G-protein subunit α-11 gene (*GNA11*) or the adaptor-related protein complex 2, sigma 1 subunit gene (*AP2S1*) causing FHH-2 and FHH-3, respectively [4-9]. The genetic cause of other, biochemically determined cases of FHH with a clear mode of autosomal dominant inheritance, remains to be determined. The CaSR is a class C, G protein coupled receptor (GPCR) consisting of an N-terminal extracellular domain, 610 amino acids in length, a classic seven transmembrane domain (amino acids 611-863) and a relatively long intracellular C-terminal tail (215 amino acids in length) [6, 10]. It is responsible for maintaining serum ionized calcium within a very narrow range (1.10–1.35 mmol/L) primarily by controlling PTH release from the parathyroid gland and calcium renal tubular reabsorption [11, 12]. The CaSR presents as a dimer on the plasma membrane with dimerization and proper

Received: 24 November 2021. **Editorial Decision:** 11 February 2022. **Corrected and Typeset:** 25 March 2022

glycosylation essential for receptor activation [13-15]. The prevalence of *CASR* variants causative of FHH has been calculated to be approximately 74 per 100 000 [16] and close to 300 variants associated with FHH have been documented; most of these are missense variants but nonsense and frameshift variants, insertions, deletions, and splice site variants have also been reported [10]. Variants have been identified in all coding regions of the *CASR* but are particularly concentrated in the Venus fly trap portion of the extracellular domain and to a lesser extent, the seven transmembrane signaling domain, including the 3 extracellular loops [10]. Only a relatively small proportion of *CASR* variants found associated with FHH have been functionally assessed.

The biochemical profile of FHH can in some cases resemble that of primary hyperparathyroidism (PHPT), a much more severe condition usually requiring exploratory neck surgery/parathyroidectomy [17, 18]. It is particularly important to distinguish between these disorders in order to avoid unwarranted surgical intervention in the case of FHH patients, in whom treatment is not normally advised. While a 24-hour renal calcium/creatinine clearance ratio (< 0.01) is recommended to distinguish FHH from PHPT, there is considerable overlap, with up to 35% of FHH patients having ratios greater than 0.01, and around 20% of patients with PHPT having ratios below this cutoff [3, 17, 18]. Hence, genetic examination for *CASR* variants (also *GNA11* and *AP2S1* variants) is a desirable course of action since such variants may be causative of FHH but are not seen in PHPT. Unless they are already well-characterized, *CASR* and other novel, genetic variants must undergo bioinformatics analysis in order to ascertain likely pathogenicity. However, it is now recognized that bioinformatics alone is insufficient to evaluate pathogenicity according to the American College of Medical Genetics (ACMG) standards and guidelines for the interpretation of gene variants [19]; in vitro functional assessment of novel variants is now considered desirable. Further substantiation of this approach in assessing pathogenicity is provided as Supplemental Data [20]. In this study we identified 3 novel *CASR* missense variants in 3 probands provisionally diagnosed with FHH and subjected them to bioinformatics analysis and functional assessment, then related these findings to their total and cell surface expression and intracellular localization, in order to guide clinical practice.

Methods

Patients, Biochemistry, and Genetic Analyses

Patients attending endocrinology clinics at Sir Charles Gairdner Hospital, Perth (patients B1, B2, and C) or the Austin Hospital, Melbourne (patient A) for suspected calcium disorders underwent a full fasting metabolic bone study, which included blood serum examination for ionized calcium; plasma analysis for intact PTH; total calcium, albumin, and creatinine; and either a urine spot (morning, second void) or 24-hour urine test, both of which included calcium and creatinine measurements. Serum, plasma, and urine biochemical analyses were performed using standard methods with calcium to creatinine clearance ratios determined as previously described [21].

Patients B1 and B2 are a father and son, both of whom are hypercalcemic. In the case of patient C, relatives were not available for biochemical or genetic evaluation to establish whether his hypercalcemia might be inherited. Patient A reportedly has a daughter who is also hypercalcemic, but biochemical or genetic data were not available for inclusion in this study.

For genetic analysis, genomic DNA extracted from blood samples was subjected to bidirectional Sanger sequencing of segments of the *CASR* encompassing exons 2 to 7, including splice donor and acceptor sites, to screen the entire coding region. Genetic analysis for patients B1, B2, and C was performed as described previously [21] while that for patient A was performed by the Molecular Genetics Department, Pathology Queensland, Brisbane, using similar methodologies. Bioinformatics analysis of *CASR* variants identified by sequence analysis was performed using wANNOVAR software [22].

All investigations were performed as part of routine clinical care with patients' consent. Ethical approval for the study was granted by the Committee for Human Rights (University of Western Australia; project ref: 05/06/004/C04).

Plasmid Construction, Mutagenesis, and Cell Transfections

Each *CASR* test variant (T699N, R701G, T808P) was introduced separately by site-directed mutagenesis (Stratagene, La Jolla, CA) into wild-type C-terminally FLAG-tagged human *CASR* cloned into the mammalian expression vector pcDNA3.1 (CaSR-FLAG/pcDNA3.1) as described previously [21, 23]. Transfection-quality plasmid DNA was generated using the Pure Yield miniprep system (Promega Corp, Madison, WI) and quantitated using a NanoDrop One spectrophotometer (Thermo Fisher Scientific, Waltham, MA). HEK293 cells (RRID: CVCL_0045, https://scicrunch.org/resolver/RRID:CVCL_0045) were cultured as described previously [23] and 25 cm^2 flasks of cells at approximately 60% confluency were transfected with 5 µg wild-type or mutant CaSR-FLAG/pcDNA3.1 (including a known inactivating control variant, L174R) or empty vector (pcDNA3.1) using Lipofectamine 2000 transfection reagent (Life Technologies, Invitrogen, Carlsbad, CA) prepared in antibiotic-free, OptiMEM medium (Invitrogen) as specified by the manufacturer. After approximately 6 hours incubation at 37 °C in 5% CO_2, the transfection medium was replaced with Dulbecco's Modified Eagle Medium (DMEM) containing 10% fetal bovine serum and antibiotics and re-incubated until required for Western blotting, immunofluorescence, or IP-One assays.

Western Blot Analysis and Immunofluorescence Studies

At 48 hours after transfection, protein was extracted using base lysis buffer (150 mM NaCl, 10 mM ethylene diamine tetra-acetic acid [EDTA], 1 mM ethylene glycol tetra-acetic acid [EGTA], 1% Triton-X-100, 20 mM Tris, pH 6.8) containing protease and phosphatase inhibitors and iodoacetamide (final concentration, 100 mM). Protein was quantitated using the bicinchoninic acid protein assay kit (Pierce, Rockford, IL) with measurements taken on a NanoDrop One spectrophotometer. Protein (100 µg for each sample) was separated on a sodium dodecyl sulfate (SDS) polyacrylamide gel prepared using a TGX Stain-Free FastCast Acrylamide Kit, 7.5% (Bio-Rad, Hercules, CA), then blotted on to nitrocellulose and probed with primary antibodies, namely, mouse monoclonals to FLAG-tag (RRID: AB_259529, https://scicrunch.org/resolver/AB_259529) to detect the CaSR and α-tubulin (RRID: AB_477593, https://scicrunch.org/resolver/AB_477593) as a loading standard, followed by goat anti-mouse-horseradish peroxidase conjugated

secondary antibody (RRID: AB_258167, https://scicrunch.org/resolver/AB_258167), with dilution/wash buffers and incubation conditions as described previously [24]. All antibodies were from Sigma-Aldrich, St Louis, MO. Bands were visualized using chemiluminescence reagent in a Molecular Imager (Bio-Rad) as described previously [21].

Immunofluorescence was performed as previously described [25]. Briefly, wild-type or variant CaSR-FLAG/pcDNA3.1-transfected HEK293 cells (48 hours posttransfection) were seeded overnight on to poly-L-lysine coated coverslips in 96-well plates, after which cells were fixed with 4% paraformaldehyde, permeabilized with 0.1% Triton X-100 and stained with antibodies against FLAG (rabbit anti-FLAG M2; RRID: AB_439687, https://scicrunch.org/resolver/RRID:AB_439687, Sigma-Aldrich), followed by anti-rabbit Alexa Fluor 488 nm (RRID: AB_2633280, https://scicrunch.org/resolver/RRID:AB_2633280, Thermo Fisher Scientific) to label the CaSR, and either rhodamine-phalloidin (Thermo Fisher Scientific) to visualize F-actin at the cell surface or protein disulfide-isomerase (PDI) antibody (RRID: AB_10615355, https://scicrunch.org/resolver/RRID:AB_10615355, Enzo Life Sciences, Villeurbanne, France) and anti-mouse Alexa Fluor 555 nm (RRID: AB_2633276, https://scicrunch.org/resolver/RRID:AB_2633276, Thermo Fisher Scientific) to visualize the endoplasmic reticulum, or anti-GM130 (Golgi matrix protein of 130 kDa) monoclonal antibody (RRID: AB_398141, https://scicrunch.org/resolver/RRID:AB_398141, BD Transduction laboratories, Franklin Lakes, NJ) to visualize the Golgi. Hoechst 33258 stain (Thermo Fisher Scientific) was used to label nuclei. Samples were mounted in ProLong Gold Antifade (Thermo Fisher Scientific) and imaged using a Nikon A1Si point scanning confocal microscope (Nikon, Tokyo, Japan) equipped with a PlanApo 100× oil objective lens (N.A. 1.45) and the images processed using Fiji software [26].

IP-One Assay, Methodology, Calculations, and Statistical Analysis

The IP-One assay which measures the accumulation of D-myo-inositol-1-phosphate following receptor activation was performed using the IP-One enzyme-linked immunosorbent assay (ELISA) kit (Cisbio Bioassays, Codolet, France; cat# 72IP1PEA, RRID:AB_2904131, https://antibodyregistry.org/search.php?q=AB_2904131) as described previously [21]. Briefly, CaSR wild-type, known inactive CaSR control, and CaSR test variant plasmids that had been transfected into HEK293 cells were seeded 8 hours later into 24-well plates (4×10^5 cells/well) and incubated for 48 hours, after which time they were washed in Ca^{++}-free DMEM, then in stimulation buffer (without calcium), and finally dosed with Ca^{++} ions in stimulation buffer (final concentrations: 0, 3, 6, and 10 mM) for 1 hour at 37 °C in 5% CO_2. Cells were then lysed and the lysate clarified by low speed centrifugation and the resultant supernatant transferred to a 96-well IP-One ELISA plate and the IP-One assay performed according to the manufacturer. Transfection/Ca^{++} stimulation experiments were performed in triplicate and IP-One assay values in duplicate. Absorbances were read on an iMark microplate absorbance reader (Bio-Rad) at 450 nm with 620 nm correction.

The 620 nm background absorbance values were subtracted from the 450 nm values for each assay point and a further correction made for nonspecific binding. Duplicate assay values were then averaged and the percentage (%) stimulation calculated as follows: % stimulation = [1 − (Absorbance$_{stim}$/Absorbance$_{nonstim}$)] × 100 where Absorbance$_{nonstim}$ is the absorbance at 0 mM Ca^{++} ions for each particular variant/control. The mean and standard error of the mean (SEM) were then calculated for each of the variants and controls and the significance of the difference in % stimulation between variant and wild-type receptor and the difference in EC_{50} value (concentration of Ca++ ions giving half maximal % stimulation) between variant and wild-type receptor assessed statistically in the R statistical computing environment, version 4.0.0.

Results

Patient Biochemistry, Variant Identification, and Bioinformatics

The relevant biochemical data for all patients was consistent with that for FHH, in particular the calcium/creatinine clearance ratios were all below 0.01 (Table 1). Serum ionized calcium and corrected plasma calcium readings were, in all cases, above the reference range and urine calcium excretion below the reference range. PTH values were mostly within the reference range, although in one case the reading was slightly elevated, which is not an uncommon finding in FHH [17]. Bidirectional Sanger sequencing confirmed the heterozygous presence of 3 different *CASR* variants in the 4 patients examined (Table 1); all variants were in the region of exon 7 encoding the transmembrane signaling domain. The variant in patient A is a cytosine to adenine transversion at nucleotide 2096, resulting in a threonine to asparagine substitution at position 699, NM_000388.4:c.2096C>A:p.(Thr699Asn) (T699N), the second variant, identified in both a father and son (B1 and B2), is a cytosine to guanine transversion at nucleotide 2101, resulting in an arginine to glycine substitution at position 701, NM_000388.4:c.2101C>G:p.(Arg701Gly) (R701G), while the third variant, in patient C, is an adenine to cytosine transversion at nucleotide 2422, resulting in a threonine to proline substitution at position 808, NM_000388.4:c.2422A>C:p.(Thr808Pro) (T808P).

All 3 nucleotide variants are novel and have not been reported in the ClinVar database. However, bioinformatics analysis referenced to databases such as PolyPhen-2, MetaLR, and FATHMM suggest that the variants are deleterious or probably/possibly damaging (Table 2), although some inconsistencies were observed between the databases in assigning pathogenicity to any particular variant. Taken together, the bioinformatics data indicate that the *CASR* 2096C>A and the 2422A>C variants are more likely to be pathogenic than the 2101C>G variant, with the SIFT and PolyPhen-2 scores for the latter designated as "tolerated" and only "possibly damaging", respectively. This is reflected in the GERP++ scores indicating that the *CASR* 2096C and 2422A alleles (both scoring 0.980) are more highly conserved than the 2101C allele (scoring 0.702). Interestingly, the combined annotation dependent depletion (CADD) scores are similar for the 3 variants but fall below the cutoff point of 30 that signifies "likely deleterious" [27].

Examination of Total and Cell Surface Expression and Intracellular Localization of CaSR Variants

Western blot analysis of CaSR variant protein expressed in HEK293 cells demonstrated that, like the control wild-type receptor and known inactivating variant receptor (L174R; 21, 23), all 3 test variants (T699N, R701G, and T808P) expressed both the immature, high mannose form of the receptor

Table 1. Patient biochemical data and *CASR* variants identified

Patient (gender)	Variant identified	Serum ionized calcium (pH 7.4) (mmol/L)	Plasma total calcium (corrected) (mmol/L)	Urine calcium excretion (#mmol/d or †µmol/L GF)	Calcium/ creatinine clearance ratio	Serum intact PTH (pmol/L)
[n] A (f)	NM_000388.4:c.2096C > A:	1.39[a]	2.75[d]	#1.85[f]	0.0052	3.2[j]
	p.(Thr699Asn)	1.46[a]	2.77[d]	#1.24[f]	0.0040	3.8[j]
[n] B1 (m)	NM_000388.4:c.2101C > G:	1.41[b]	2.64[d]	†2.0[g]	0.0008	8.2[k]
B2 (m)	p.(Arg701Gly)	1.44[c]	2. 67[e]	†12.0[h]	0.0047	6.4[l]
[n] C (m)	NM_000388.4:c.2422A > C: p.(Thr808Pro)	1.47[b]	2.65[d]	†9.0[i]	0.0034	4.8[m]

Serum ionized calcium (pH 7.4): Reference range (mmol/L) =
[a]1.13-1.32,
[b]1.12-1.32,
[c]1.12-1.30.
Plasma total calcium (corrected): Reference range (mmol/L) =
[d]2.15-2.55,
[e]2.10-2.60.
Urine calcium excretion: Reference range =
[f]2.5-7.5 mmol/d; or
[g]34-115,
[h]32-111,
[i]35-120 µmol/L GF.
Calcium/creatinine clearance ratio (< 0.01 indicative of FHH as opposed to PHPT).
Serum intact PTH: Reference range (pmol/L) =
[j]1.6-6.0,
[k]1.6-6.9,
[l]1.9-8.5,
[m]0.9-9.0.
[n]Signifies the proband; the 2 sets of readings for patient A were taken approximately 4 months apart; patient B1 is the father of B2.

Table 2. Bioinformatics data for the 3 novel test *CASR* gene variants

Variant	SIFT score	PolyPhen-2 HVAR score	CADD Phred score	MetaLR score	Mutation assessor rank score	FATHMM converted rank score	GERP++ RS rank score	SiPhy SiPhy 29way logOdds rank score
NM_000388.4:c.2096C>A: p.(Thr699Asn)	deleterious (0.001)	probably damaging (0.998)	likely benign (26.5)	deleterious (0.908)	medium (0.729)	deleterious (0.901)	0.980	0.954
NM_000388.4:c.2101C>G: p.(Arg701Gly)	tolerated (0.329)	possibly damaging (0.721)	likely benign (26.9)	deleterious (0.834)	medium (0.819)	deleterious (0.905)	0.702	0.769
NM_000388.4:c.2422A>C: p.(Thr808Pro)	deleterious (0.001)	probably damaging (0.956)	likely benign (24.6)	deleterious (0.894)	high (0.952)	deleterious (0.896)	0.980	0.777

Note that as the test variants are novel, their population frequencies are not able to be determined. The combined annotation dependent depletion (CADD) score cutoff for "likely deleterious" is > 30 [27].

(140 kDa) and the mature glycosylated form (160 kDa) [28], with the amount of immature receptor similar for the control and test variants, except for T808P which was somewhat lower than the others (Fig. 1). However, all the test variants displayed reduced levels of the mature receptor compared with the wild-type receptor; notably the approximate ratio of mature to immature receptor was greater for the wild-type compared with the test variants and control L174R variant. This suggests that reduced expression of mature receptor might translate to reduced cell surface expression for the variant receptors.

To assess the cell surface expression of the CaSR test variants, we next performed immunofluorescence confocal microscopy using rhodamine-phalloidin (F-actin) to label the cell surface and compared the surface localization of each variant against the wild-type receptor as well as 2 known inactivating control variants, L174R and G509R [21] (Fig. 2A). The G509R variant was included as a cell surface "negative control" as it does not produce mature glycosylated receptor and thus is purportedly retained in the endoplasmic reticulum (ER) [21]. As expected, the wild-type receptor displayed considerable cell surface localization as indicated by the strong colocalization (yellow) upon merger of the CaSR (green) and F-actin (red) fluorescent signals (Fig. 2A, top right panel, arrowed), whereas the negative control G509R receptor was almost exclusively retained intracellularly, where it was concentrated toward the perinuclear region and occupied a lattice-like network reminiscent of the ER (Fig. 2A, row 3 panels, dashed arrows). By comparison, the LI74R control and the 3 novel test variants all exhibited varying degrees of cell surface labeling, but these levels were visibly lower than that for the wild-type receptor, as indicated by the reduced colocalization signal between the variants and F-actin (yellow color in merged images, unbroken arrows). In addition to the cell surface, the localization of variants L174R, T699N, and R701G extended to lattice-like and globular intracellular compartments (Fig. 2A, rows 2, 4, and 5 panels, dashed arrows).

To define these compartments, we next assessed the subcellular localization of the variant and control receptors by immunofluorescence confocal microscopy using well-established organelle markers against the ER (PDI, Fig. 2B), and the Golgi (GM130, data not shown). As expected, the G509R receptor, but not the wild-type, strongly colocalized with PDI, thus confirming its sequestration to the ER (Fig. 2B, row 3 panel, merged, arrowed). The test receptors all showed some degree of colocalization with the ER, T699N > L174R > T808P > R701G, albeit to a lesser extent compared to the G509R negative control receptor (Fig. 2B, rows 2 to 6 panels, merged, arrowed). In some instances, the test variants were also observed to localize to a perinuclear globular Golgi-like structure (eg, R701G in Fig. 2A, dashed arrows). However, this structure failed to colocalize with the Golgi marker GM130 (data not shown) indicating that it was unlikely to be of Golgi origin and instead might reflect protein aggregation upon ectopic expression of the CaSR variants in HEK293 cells. Overall, intracellular retention of the CaSR was greater for the variant receptors compared with wild-type, suggesting impairments in intracellular processing and/or trafficking of the CaSR variants to the cell surface.

Analysis of CaSR Variant Activation and Resulting Pathogenicity Status

The wild-type receptor responded to Ca^{++} stimulation in a dose-dependent manner, while the known inactivating receptor (L174R) showed virtually no response to any concentration of Ca^{++} ions in keeping with results from previous studies [21]. The dose response curve for each of the test receptors was right-shifted compared with the wild-type receptor, indicating that all test variants are inactivating (Fig. 3A). At a concentration of 3 mM (closest to physiological levels), the % stimulation was significantly diminished for all 3 test receptors compared to the wild-type receptor ($P \leq 0.001$), whereas at supraphysiologic levels (10 mM) the activation was significantly reduced only for the T808P and T699N receptors ($P \leq 0.001$), where the mean maximal % stimulation values were less than half the mean maximal value for the wild-type receptor, but higher than that for the control inactivating receptor, L174R (Fig. 3B). We also compared the mean EC_{50} values for wild-type and the 3 test variant receptors; the EC_{50} values for the R701G and T699N receptors (2.6 mM and 3.8 mM, respectively) were higher than that for the wild-type receptor (1.1 mM) ($P = 0.022, 0.011$); however, after Bonferroni correction for multiple testing the difference between the R701G and wild-type receptor was not significant ($P > 0.017$) (Fig. 3C). The difference between the mean wild-type and T808P EC_{50} values (1.1 mM and 1.9 mM, respectively) was not significant ($P = 0.346$).

We assessed the pathogenic status of each of the test variants before and after functional analysis using the University of Maryland School of Medicine's Genetic Variation Interpretation Tool as outlined by Richards et al [19]; all 3 variants were classified as "Variants of Unknown Significance" (VUS) before functional analysis, but were classified as "Likely Pathogenic II" after the functional analysis which demonstrated that they were inactivating.

Discussion

In this study, we characterized 3 variants of the *CASR* detected in 4 hypercalcemic individuals from 3 kindreds. In each case, the clinical presentation was consistent with FHH: the 4 affected individuals had mild hypercalcemia, unsuppressed PTH, and marked renal calcium conservation, and in 2 kindreds there was a family history of hypercalcemia. However, given the known overlap between biochemical findings in FHH and PHPT, the alternative diagnosis of PHPT was not excluded. Genetic sequencing of the *CASR* gene detected 3 novel variants. Bioinformatics analysis gave somewhat conflicting results but suggested that the variants were likely to be deleterious at least when referenced to some databases, with the 2096C>A and 2422A>C variants more likely to be damaging than the 2101C>G variant, the latter classified as tolerated (SIFT score) and only possibly damaging (PolyPhen-2 HVAR score). Interestingly, a 2102G>C nucleotide variant affecting the 701 codon and leading to a R701P amino acid substitution [29] demonstrated similar bioinformatics scores to the 2101C>G variant apart from the PolyPhen 2 HVAR score (0.948) which placed the 2102G>C variant in the "probably damaging" category. Overall, based on bioinformatics analysis alone, all 3 variants were classified as "Variants of Unknown Significance", meaning that in clinical practice the diagnosis of FHH remained unconfirmed. Functional studies were therefore required to progress the differential diagnosis and establish whether the *CASR* variants were pathogenic. For all 3 variants, Western blot analysis and immunofluorescence studies demonstrated impaired expression of mature receptor reaching the cell surface and

the IP-One assay revealed diminished receptor activation at physiologically relevant Ca^{++} concentrations. Application of the genetic variation interpretation tool to the variants following functional assessment permitted classification of each as "Likely Pathogenic II," thus firming up the diagnosis of FHH in individuals with these variants.

The bioinformatics data suggesting that the R701G variant may be a milder inactivating variant than the other 2 variants is supported by the Western blot analysis, which demonstrated that the R701G variant has proportionally greater mature 160 KDa receptor than the other 2 variants, and the immunofluorescence studies that show relatively higher levels of cell surface R701G receptor compared with the other test variants. In addition, the R701G receptor showed a higher % stimulation at all levels of Ca^{++} tested compared to the other 2 variants; nevertheless, R701G receptor activation is significantly below that for the wild-type receptor at physiologically relevant Ca^{++} concentrations and there is no appreciable difference in the calcium biochemistry of the patients harboring this variant compared to those with the other 2 variants. Notwithstanding this, all 3 variants, when expressed in HEK293 cells and examined by Western blot analysis, demonstrated a lower ratio of mature receptor to total receptor compared with the wild-type CaSR. Dersham et al [16] also found significantly reduced mature receptor in 12 *CASR* loss-of-function variants, while plasma membrane localization was also significantly reduced for all 12 of these variants compared with wild-type receptor. Interestingly, this study also found that 2 gain-of-function *CASR* variants demonstrated significantly elevated levels of mature receptor and plasma membrane localization compared with the wild-type receptor. Other studies have also shown that missense variant CaSRs associated with FHH are impaired with regard to maturation, cell surface expression, and signaling capacity compared with the wild-type receptor [30]

The Western blot analysis is complemented by our immunofluorescence results, which show much higher levels of cell surface receptor in the HEK293 cells expressing wild-type receptor compared to the variants. Indeed, the variants were more likely to colocalize with the ER in lattice-like arrays or globular forms, although they each expressed receptor on the cell surface to varying degrees. By contrast, the G590R variant, which we previously confirmed as a CaSR variant causing FHH and expressed only in the immature form [21], appears to exclusively colocalize with the ER marker, indicating that it remains sequestered within the ER, possibly due to an inability to fold correctly. These results and others [16, 30] suggest that inadequate processing of the receptor to a form that can reach the cell surface and undergo ligand stimulation is a likely contributing factor to the inactivating nature of many of the variants associated with FHH. In this respect, the FHH phenotype might largely be due to reduced receptor numbers on the cell surface as has been demonstrated in an earlier mouse model [31]. Inadequate processing may, in part, be due to deficiencies in the variants passing conformational control checks in the ER [32]. We have recently shown that the ER quality control protein, osteosarcoma-9 (OS-9), binds exclusively to immature (presumably misfolded) CaSR when directed to the ER [33] and it will be of interest to determine whether enhanced binding of OS-9 to the G590R variant, as well as some of the other loss-of-function variants, occurs when compared with wild-type receptor. The inability to detect wild-type CaSR colocalization in the Golgi was somewhat surprising, as it is known that mature glycosylation of the receptor occurs here [34]; however, it likely reflects the transitory nature of receptor processing in this organelle. The immunofluorescence data strengthens this study over many others examining missense *CASR* variants, by demonstrating that the reduction in mature variant receptor compared to wild-type (as seen by Western blot analysis) translates to a considerable reduction in mature receptor actually reaching the cell surface.

The 3 variants under investigation are all located in the transmembrane (TM) domain of the CaSR: T699N and R701G in TM3 in close proximity to the amino-terminal end of intracellular loop 2 (ICL-2), and T808P in TM6 in close proximity to the carboxy-terminal end of ICL-3 [10]. The T699N and R701G variants would seem to form part of a cluster of variants in this region of TM3 that are associated with FHH [10] while variants affecting residues either side of T808P in TM6 (namely I807N, F809I, F809L) are also associated with FHH, likewise forming a cluster of inactivating variants in this region [10, 35, 36]. In other class C GPCRs, TM3 and TM6 undergo conformational changes that are critically important for agonist-induced G-protein mediated signaling [37]. This includes an "ionic lock" mechanism involving residues from the intracellular ends of TM3 and TM6 [38] and mechanisms by which dimers reorientate from the inactive TM5, TM4/TM5, or TM3/TM4 interface to an active TM6 interface with a conserved TM6 toggle switch stabilizing the active conformation in class C GPCRs such as the metabotropic

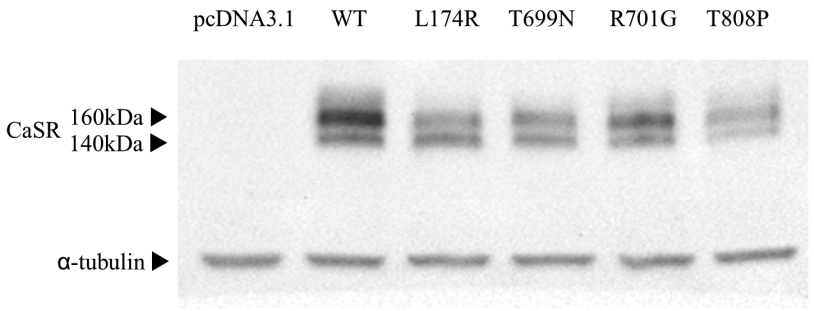

Figure 1. Western blot analysis demonstrating CaSR wild-type, control inactivating variant (L174R) and test variant (T699N, R701G, T808P) expression in HEK293 cells. Empty vector (pcDNA3.1) was included as a background control. Plasmid DNA was transfected into HEK293 cells and 48 hours later, the cells lysed and the protein (100 µg) separated on a 7.5% polyacrylamide gel, then blotted on to nitrocellulose and probed with anti-FLAG antibody to detect CaSR mature (160 kDa) and immature (140 kDa) forms and with anti-α-tubulin antibody as a loading control.

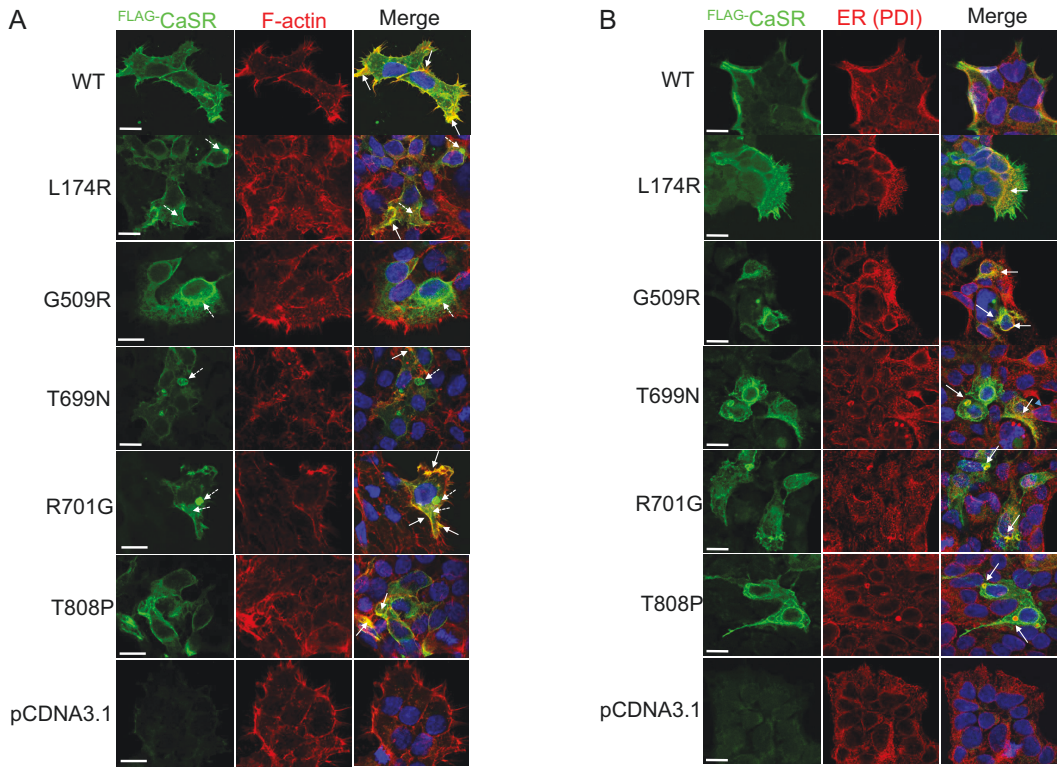

Figure 2. Fluorescence confocal microscopy examination of wild-type, control inactivating variants (L174R and G509R), and test variants (T699N, R701G, T808P) in HEK293 cells. A, cell surface expression. B, ER localization. Empty vector (pcDNA3.1) was included as a background control in both experiments. Plasmid DNA was transfected into HEK293 cells and 48 hours later seeded on to coverslips and after overnight culture, cells were fixed, permeabilized and probed with anti-FLAG Alexa Fluor 488 nm antibody to detect the CaSR (left panels, green) and either stained with rhodamine-phalloidin to detect the cell surface marker, F-actin (A, central panels, red) or anti-PDI Alexa Fluor 555 nm antibody to detect the ER (B, central panels, red). Nuclei were identified using Hoechst 33258 stain and the cells imaged using a Nikon-A1Si point scanning confocal microscope. Merged images are shown in the right-hand side panels for both A and B. White unbroken arrows (A, merged) indicate examples of strong cell surface localization of receptor, whereas white broken arrows (A, left and right panels) demonstrate receptor localization in globular-like structures or lattice-like arrays. For (B) white unbroken arrows (B, merged) identify regions of receptor colocalization in the ER, either in globular compartments or lattice-like arrays.

glutamate and $GABA_B$ receptors [39-42]. Recent cryo–electron microscopic analysis of the inactive and active structure of near full length CaSR (including the TM domain) in the presence or absence of various allosteric modulators has confirmed the critical importance of TM6 in receptor activation and G protein coupling [43]. In particular, activation of the CaSR homodimer causes an asymmetric orientation of the TM6-TM6 interface with the conserved toggle switch motif (Tryp818–Pro823) playing a crucial role in stabilizing this conformation. In addition, this conformational change creates a space that is able to accommodate compounds such as cholesterol hemisuccinate, the presence of which could be further stabilized by the cholesterol-binding CARC motif (Lys805–Leu812) observed in TM6. This has implications for the binding of the CaSR to cholesterol-rich caveolae, the site of CaSR-mediated signal transduction in parathyroid cells [44]. The presence of the T808P variant in TM6 suggests that it might disrupt TM6 interface orientation leading to diminished signal transduction, while its presence directly within the CARC motif indicates that it could interfere with binding to caveolae thus compromising signaling capacity by a different means. While the cryo-electron microscopic analysis of the CaSR failed to elucidate the presence of an ionic lock type mechanism involving TM3, the high number of inactivating variants detected in this domain, including the 2 confirmed in this study, would suggest that TM3 plays an important role either in relaying conformational changes to the TM6 interface or in allowing G protein coupling to occur. In support of the latter, cryo-electron microscopic studies of the CaSR suggest that G protein coupling is facilitated by downward extensions of both ICL-2 and the C terminus of the protomer to which it binds ([43]; supplementary data, Fig. 9). The close proximity of the variants T699N and R701G to ICL-2 suggests that they could interfere with ICL-2's downward extension to accommodate G protein coupling.

In summary, we confirmed by in vitro studies the inactivating nature of 3 novel *CASR* missense variants identified in patients with a biochemical profile consistent with FHH, but with insubstantial family studies demonstrating co-segregation of the variant with the disorder, and an ambiguous bioinformatics assessment of pathogenicity. These results underscore the importance of functional assessment of *CASR* variants associated with FHH and other CaSR-related disorders in assigning pathogenicity. All variants are located in the heptahelical TM domain of the receptor and, while inactivation may be due wholly or in part to reduced cell surface expression exhibited by the variants, it may also be caused by conformational changes in the TM domains induced by the variants that affect their stability and G-protein coupling or by alterations that affect binding to caveolae. With the ever-increasing availability of genetic testing in clinical practice, "variants of unknown significance" are now often encountered by clinicians; however, such classification causes further frustration and does little to aid the diagnosis. This study

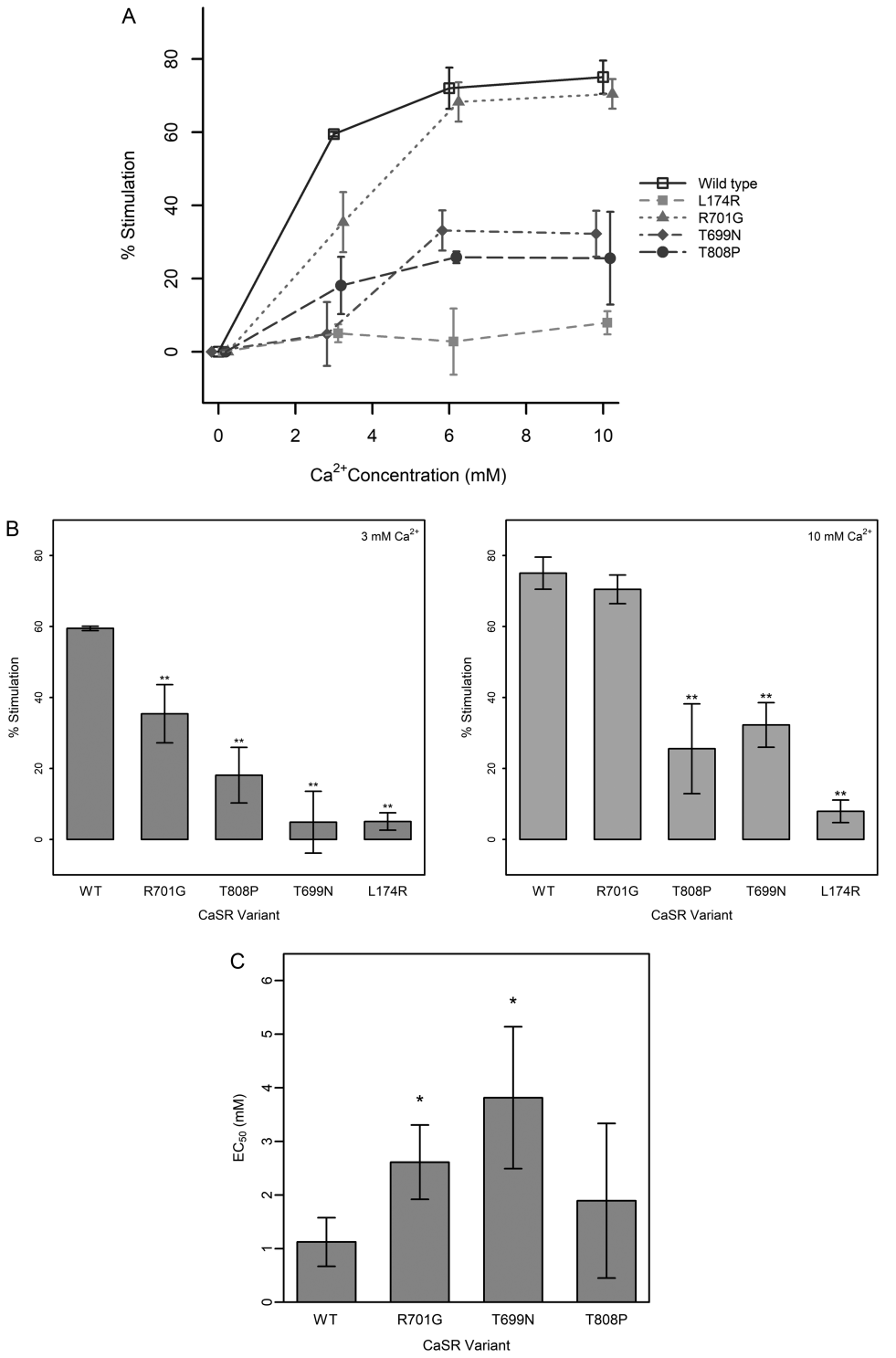

Figure 3. Comparative analysis of receptor activation following Ca^{++} stimulation for wild-type, control inactivating (L174R), and test variant (T699N, R701G, T808P) receptors using the IP-One ELISA assay. HEK293 cells were transfected with plasmid DNA, 8 hours later seeded into 24-well plates, and the following day dosed with varying concentrations of Ca^{++}, after which the cells were lysed and examined for D-myo-inositol-1-phosphate accumulation using the IP-One ELISA assay. A, Dose response curves plotting mean % stimulation (± 2× SEM error bars) against Ca^{++} ion concentration for 3 experiments for wild-type, control inactivating, and test receptors. B, Bar plots representing comparative % stimulation of wild-type, control inactivating, and test variant receptors at Ca^{++} concentrations of 3 mM or 10 mM; bars represent the mean % stimulation (± 2× SEM error bars) for 3 experiments with $^{**}P$ value = < 0.001 (compared to wild-type receptor % stimulation). C, Bar plot comparing the EC_{50} values for wild-type receptor with those for the 3 test receptors; bars represent the mean EC_{50} (± 2× SEM error bars) for 3 experiments; $^{*}P$ value < 0.05 (compared to wild-type receptor EC_{50}).

demonstrates the importance of functional laboratory studies in assessment of such variants, which assists in confirming or refuting clinical diagnoses with clear implications for patient care, in particular the avoidance of unnecessary exploratory neck surgery or parathyroidectomy for suspected PHPT, as has been observed in the past [45].

Acknowledgments

We thank Drs. Warwick Howe and Ken Paton (Perth) and Stephen Farrell, Suresh Varadarajan, and Anna Lever (Melbourne) for clinical/genetic consultation regarding patients whose *CASR* variants were examined in this study. We also thank staff at the Australian Genome Research Facility (Perth) and Pathology Queensland (Brisbane) for help with patient genetic testing/analysis. All microscopy was carried out using facilities at the Centre for Microscopy, Characterisation, and Analysis, University of Western Australia.

Financial Support

This study was supported by a grant from the Sir Charles Gairdner Osborne Park Health Care Group Research Advisory Committee, Funding Round 2019 (Grant number: RAC2019-20/029) and, in part, by funding from the National Health and Medical Research Council of Australia (APP2003629 to B.H.M and APP1078280 to N.J.P) and a Department of Health (Western Australia) Merit Award (No. 1186046 to B.H.M).

Disclosures

None of the authors have anything to disclose in relation to this manuscript. All authors have no reported conflicts of interest. All authors have submitted the ICMJE Form for Disclosure of Potential Conflicts of Interest.

Data Availability

Some or all of the datasets generated and/or analyzed during the current study are not publicly available but are available from the corresponding author by request.

References

1. Ward BK, Magno AL, Walsh JP, *et al*. The role of the calcium-sensing receptor in human disease. *Clin Biochem*. 2012;45(12):943-953.
2. Marx SJ. Calcimimetic use in familial hypocalciuric hypercalcemia – a perspective in endocrinology. *J Clin Endocrinol Metab*. 2017;102(11):3933-3936.
3. Mannstadt M. Disorders of the calcium-sensing receptor - familial hypocalciuric hypercalcemia and autosomal dominant hypocalcemia. In: Rosen CJ, Mulder JE, eds. *UpToDate*. UpToDate; 2021. Accessed October 20, 2021. www.uptodate.com
4. Magno AL, Ward BK, Ratajczak T. The calcium-sensing receptor: a molecular perspective. *Endocr Rev*. 2011;32(1):3-30.
5. Brown EM, Gamba G, Riccardi D, *et al*. Cloning and characterization of an extracellular Ca^{2+}-sensing receptor from bovine parathyroid. *Nature* 1993;366(6455):575-580.
6. Garrett JE, Capuano IV, Hammerland LG, *et al*. Molecular-cloning and functional expression of human parathyroid calcium receptor cDNAs. *J Biol Chem*. 1995;270(21):12919-12925.
7. Pollak MR, Brown EM, Chou YH, *et al*. Mutations in the human Ca(2+)-sensing receptor gene cause familial hypocalciuric hypercalcemia and neonatal severe hyperparathyroidism. *Cell*. 1993;75(7):1297-1303.
8. Nesbit MA, Hannan FM, Howles SA, *et al*. Mutations affecting G-protein subunit α11 in hypercalcemia and hypocalcemia. *New England J Med*. 2013;368(26):2476-2486.
9. Nesbit MA, Hannan FM, Howles SA, *et al*. Mutations in *AP2S1* cause familial hypocalciuric hypercalcemia type 3. *Nat Genet*. 2013;45(1):93-97.
10. Gorvin CM. Molecular and clinical insights from studies of calcium-sensing receptor mutations. *J Mol Endocrinol*. 2019;63(2):R1-R16. doi:10.1530/JME-19-0104
11. Peacock M. Calcium metabolism in health and disease. *Clin J Am Soc Nephrol*. 2010;5(Supplement 1):S23-S30.
12. Brown EM. Role of the calcium-sensing receptor in extracellular calcium homeostasis. *Best Pract Res Clin Endocrinol Metab*. 2013;27(3):333-343.
13. Bai M, Trivedi S, Kifor O, *et al*. Intermolecular interactions between dimeric calcium-sensing receptor monomers are important for its normal function. *Proc Natl Acad Sci USA*. 1999;96(6):2834-2839.
14. Zhang Z, Sun S, Quinn SJ, *et al*. The extracellular calcium-sensing receptor dimerizes through multiple types of intermolecular interactions. *J Biol Chem*. 2001;276(7):5316-5322.
15. Ray K, Clapp P, Goldsmith P, Spiegel A. Identification of the sites of *N*-linked glycosylation on the human calcium receptor and assessment of their role in cell surface expression and signal transduction. *J Biol Chem*. 1998;273(51):34558-34567.
16. Dersham R, Gorvin CM, Raghu PR, *et al*. Familial hypocalciuric hypercalcemia type 1 and autosomal-dominant hypocalcemia type 1: prevalence in a large healthcare population. *Am J Human Genet*. 2020;106(6):734-747.
17. Lee JY, Shoback DM. Familial hypocalciuric hypercalcemia and related disorders. *Best Practice Res Clin Endocrinol Metab*. (2018)2018;32(5):609-619.
18. Stuckey BGA, Kent GN, Gutteridge DH, *et al*. Fasting calcium excretion and parathyroid hormone together distinguish familial hypocalciuric hypercalcaemia from primary hyperparathyroidism. *Clin Endocrinol*. 1987;27(5):525-533.
19. Richards S, Aziz N, Bale S, *et al*. Standards and guidelines for the interpretation of sequence variants: a joint consensus recommendation of the American College of Medical Genetics and Genomics and the Association for Molecular Pathology. *Genet Medicine*. 2015;17(5):405-423.
20. Ward B. Supplemental bioinformatics data. *Figshare*. Deposited January 19, 2022. https://doi.org/10.6084/m9.figshare.18699752.v1
21. Magno AL, Leatherbarrow KM, Brown SJ, *et al*. Functional analysis of calcium-sensing receptor variants identified in families provisionally diagnosed with familial hypocalciuric hypercalcaemia. *Calcif Tissue Int*. 2020;107(3):230-239.
22. Wang K, Li M, Hakonarson H. ANNOVAR: functional annotation of genetic variants from high-throughput sequencing data. *Nucl Acids Res*. 2010;38(16):e164.
23. Ward BK, Magno AL, Blitvich BJ, *et al*. Novel mutations in the calcium-sensing receptor gene associated with biochemical and functional differences in familial hypocalciuric hypercalcaemia. *Clin Endocrinol*. 2006;64(5):580-587.
24. Arulpragasam A, Magno AL, Ingley E, *et al*. The adaptor protein 14-3-3 binds to the calcium-sensing receptor and attenuates receptor-mediated Rho kinase signalling. *Biochem J*. 2012;441(3):995-1006.
25. Chan ASM, Clairfeuille T, Landao-Bassonga, *et al*. Sorting nexin 27 couples PTHR trafficking to retromer for signal reduction in osteoblasts during bone growth. *Mol Biol Cell*. 2016;27(8):1367-1382.
26. Schindelin J, Arganda-Carreras I, Frise E, *et al*. Fiji – an open source platform for biological image analysis. *Nat Methods*. 2012;9(7):676-682. doi:10.1038/nmeth.2019.
27. Howe KL, Achuthan P, Allen J, *et al*. Ensembl 2021. *Nucleic Acids Res*. 2021;49(D1):D884-D891.
28. Bai M, Quinn S, Trevedi S, *et al*. Expression and characterization of inactivating and activating mutations in the human Ca^{2+} *o*-sensing receptor. *J Biol Chem*. 1996;271(32):19537-19545.
29. Hannan FM, Nesbit MA, Zhang C, *et al*. Identification of 70 calcium sensing receptor mutations in hyper- and hypo-calcaemic patients: evidence for clustering of extracellular domain mutations at calcium-binding sites. *Hum Mol Genet*. 2012;21(12):2768-2778.
30. Guarnieri V, Canaff L, Yun FHJ, *et al*. Calcium-sensing receptor (*CASR*) mutations in hypercalcaemic states: studies from a single

endocrine clinic over three years. *J Clin Endocrinol Metab*. 2010;95(4):1819-1829.
31. Ho C, Conner DA, Pollak MR, *et al*. A mouse model of human familial hypocalciuric hypercalcemia and neonatal severe hyperparathyroidism. *Nat Genet*. 1995;11(4):389-394. doi:10.1038/ng1295-389.
32. Huang Y, Breitwieser GE. Rescue of calcium-sensing receptor mutants by allosteric modulators reveals a conformational checkpoint in receptor biogenesis. *J Biol Chem*. 2007;282(13):9517-9525.
33. Ward BK, Rea SL, Magno AL, *et al*. The endoplasmic reticulum-associated protein, OS-9, behaves as a lectin in targeting the immature calcium-sensing receptor. *J Cell Physiol*. 2018;233(1):38-56.
34. Bouschet T, Martin S, Henley JM, *et al*. Receptor-activity-modifying proteins are required for forward trafficking of the calcium-sensing receptor to the plasma membrane. *J Cell Sci*. 2005;118(471):4709-4720.
35. Timmers HJLM, Karperien M, Hamdy NAT, *et al*. Normalization of serum calcium by cinacalcet in a patient with hypercalcaemia due to a *de novo* inactivating mutation of the calcium-sensing receptor. *J Intern Med*. 2006;260(2):177-182.
36. Vargas-Poussou R, Mansour-Hedili L, Baron S, *et al*. Familial hypocalciuric hypercalcemia types 1 and 3 and primary hyperparathyroidism: similarities and differences. *J Clin Endocrinol Metab*. 2016;101(5):2185-2195.
37. Ellaithy A, Gonzalez-Maeso J, Logothetis DA, *et al*. Structural and biophysical mechanisms of class C G protein-coupled receptor function. *Trends Biochem Sci*. 2020;45(12):1049-1064.
38. Binet V, Duthey B, Lecaillon J, *et al*. Common structural requirements for heptahelical domain function in class A and class C G protein-coupled receptors. *J Biol Chem*. 2007;282(16):12154-12163.
39. Xue L, Rovira X, Scholler P, *et al*. Major ligand-induced rearrangement of the heptahelical domain interface in a GPCR dimer. *Nature Chem Biol*. 2015;11(2):134-140.
40. Xue L, Sun Q, Zhao H, *et al*. Rearrangement of the transmembrane domain interfaces associated with the activation of a GPCR hetero-oligomer. *Nature Commun*. 2019;10(1):2765
41. Dore AS, Okrasa K, Patel JC, *et al*. Structure of class C GPCR metabotropic glutamate receptor 5 transmembrane domain. *Nature*. 2014;511(7511):557-562. doi:10.1038/nature13396
42. Seven AB, Barros-Alvarez X, de Lapeyriere M, *et al*. G-protein activation by a metabotropic glutamate receptor. *Nature*. 2021;595(7867):450-454.
43. Gao Y, Robertson MJ, Rahman SN, *et al*. Asymmetric activation of the calcium-sensing receptor homodimer. *Nature*. 2021;595(7867):455-459.
44. Kifor O, Diaz R, Butters R, *et al*. The calcium-sensing receptor is localized in caveolin-rich plasma membrane domains of bovine parathyroid cells. *J Biol Chem*. 1998;273(34):21708-21713.
45. Maltese G, Izatt L, McGowan BM, *et al*. Making (mis) sense of asymptomatic marked hypercalcemia in pregnancy. *Clin Case Rep* 2017;5(10):1587-1590. doi:10.1002/ccr3.1074